Median Nerve Stimulation Induces Long-Latency Gamma Modulation in the Somatosensory Cortex that Contrasts States of Consciousness

Authors' Names and Degrees:

Priscella Asman, PHD[1], Giuseppe Pellizzer, PHD[2], Sudhakar Tummala, MD[3], Israt Tasnim, BSc[1], Dhiego Bastos MD[3], Shreyas Bhavsar, DO[4], Sujit Prabhu, MD[3], and Nuri F. Ince, PHD[1*]

Current Affiliation:

Biomedical Engineering Department, University of Houston, Houston, TX, USA 1

Research Service, Minneapolis VA Health Care System, and Departments of Neurology, and of Neuroscience, University of Minnesota, Minnesota, MN, USA 2

Department of Neurosurgery, UT MD Anderson Cancer Center, Houston, TX, USA 3

Department of Anesthesiology and Perioperative Medicine, UT MD Anderson Cancer Center, Houston, TX, USA 4

Post-Publication Corresponding Author:

*Corresponding Author: nfince@uh.edu

Funding and Disclosures:

This study was supported by grants from the National Institutes of Health—National Institute of Neurological Disorders and Stroke (R01NS112497, UH3NS117944) and the National Science Foundation (2124705). GP was supported by the United States Department of Veterans Affairs Clinical Sciences Research and Development Merit Review Award 5I01CX001773-02 and by the United States Department of Veterans Affairs Rehabilitation Research and Development Pilot Project I21 RX003007.

Acknowledgments: The authors are indebted to the eight patients and the neurological team of MD Anderson who made this work possible.

Conflict of Interest Statement: None of the authors have potential conflicts of interest to be disclosed

Abstract:

Objective: To evaluate the functional use of sub-band modulations in somatosensory evoked potentials (SSEPs) to discriminate between the primary somatosensory (S1) and motor (M1) areas and contrast the states of consciousness.

Method: During routine intraoperative cortical mapping, SSEPs were recorded with electrocorticography (ECoG) grids from the sensorimotor cortex of eight patients in the anesthetized and awake states. We conducted a time-frequency analysis on the SSEP trace to extract the spectral modulations in each state and visualize their spatial topography.

Results: We observed late gamma modulation (60-250Hz) in all subjects approximately 50ms after stimulation onset, extending up to 250ms in each state. The late gamma activity enhancement was predominant in S1 in the awake state, where it discriminated S1 from M1 at a higher accuracy (92%) than in the anesthetized state (accuracy = 70%).

Conclusion: These results showed that sensorimotor mapping does not need to rely on only SSEP phase reversal. The long latency gamma modulation can serve as a biomarker for primary sensorimotor localization and monitor the level of consciousness in neurosurgical practice.

Significance: While the intraoperative assessment of SSEP phase reversal with ECoG is widely employed to delineate the central sulcus, the median nerve stimulation-induced spatio-spectral patterns can distinctly localize it and distinguish between conscious states.

Highlights:

- The median nerve induced SSEPs contain spectral features in the gamma range that can delineate the CS, along with its temporal features as a heat map.
- The SSEP's long latency gamma activity is focal to S1 in the awake state.
- The SSEP's long latency gamma activity is suppressed in the anesthetized state and enhanced in the awake state.

Keywords: Somatosensory Evoked Potentials, Cortical Mapping, ECoG, Gamma Band, Consciousness

1. Introduction:

Short-latency somatosensory evoked potentials (SSEPs) in electrocorticogram (ECoG) are commonly used to delineate the central sulcus (CS) in sensorimotor mapping during neurosurgery (Cedzich et al. 1996, Gross et al. 2000, Sheth et al. 2013). After stimulation onset, SSEPs at the boundaries of the CS are characterized by posterior/somatosensory negative and anterior/motor positive peaks at about 20ms (N20 and P20, respectively) (Nuwer et al. 1991, Pondal-Sordo et al. 2006, Endisch et al. 2015, Oh et al. 2019). Consequently, the stimulation-locked phase reversal in SSEP provides relevant information about the location of the CS (Friedman et al. 1988, Woolsey et al. 1979). This technique has been used for decades to delineate the eloquent sensorimotor cortex (Kombos et al. 2001, Gobbele et al. 2004, Duffau et al. 2005, Endisch et al. 2015, Lavrador et al. 2021).

In the spectral domain, SSEPs contain components in the gamma range (60-250Hz). An earlier study showed that somatosensory-induced gamma modulation from 15ms to 60ms emerged in the post-central gyrus (Fukuda et al. 2008). While these studies showed that the induced spectral modulations help identify the primary somatosensory area (S1) for sensorimotor mapping, they did not investigate spectral activity in the gamma range beyond 60ms (Allison et al. 1989, Fukuda et al. 2008). Therefore, it remains unclear whether somatosensory-induced long-latency spectral modulations in the gamma range in S1 exist.

Furthermore, studies of the effects of anesthesia on SSEPs that could be useful in evaluating the level of consciousness have shown contradicting results. While some studies have observed significant alterations in N20 amplitude between anesthetized and awake states (Banoub et al. 2003, Burnos et at. 2016), other studies did not find any significant differences in N20 amplitude (Bala et al. 2008, Tobias et al. 2008, Hasan et al. 2018). Earlier work suggests that late gamma band modulation in visual evoked potentials are consistent predictors of the conscious state in contrast to early potentials (Sergent et al. 2005). At this point, it is still unknown whether SSEPs include any late-onset modulation in the gamma range and whether they can distinguish the conscious state.

In the present study, cortical activity related to electrical stimulation of the median nerve was recorded with ECoG grids on eight patients during their craniotomy in the anesthetized and awake states to assess the spectral characteristics of the SSEP trace. We tested the feasibility of using

induced spectral modulations over a time window of 250 ms to assist in defining the sensorimotor region and to discern awake from anesthetized states.

Consistently in all subjects, we found late gamma power increase starting 50ms after the stimulation onset in the awake/conscious state that was highly focal in S1. We expect that, along with the phase-locked evoked activity, induced gamma modulation can be used as a strategic tool for functional mapping and for assessing the level of consciousness.

2. Methods

2.1 Patients

Eight patients (4 males and 4 females, ages 20-50 years) scheduled for resection surgeries requiring an awake craniotomy were recruited in this study. The inclusion criteria consisted of patients with primary brain tumors within or adjacent to the peri-Rolandic area. The area of tumor infiltration is indicated for each patient in Table 1.

The protocol included using high-density ECoG recording for real-time cortical mapping and CS delineation by assessing the median nerve SSEPs during the anesthetized and awake states. The study protocol was reviewed and approved by the Institutional Review Board (IRB). Each patient was made aware of the characteristic thumb twitching they would experience from the median nerve stimulation a day before their surgery. They consented to undergo the cortical mapping and to participate in this study.

2.2 Surgical procedure and anesthesia administration

The anesthetic management was conducted using the asleep-awake-asleep technique (Huncke et al. 1998). In this three-part procedure, after being administered general anesthesia for the surgical craniotomy and dural opening, each patient emerged from anesthesia for clinical neurological monitoring. The general anesthesia for these procedures was administered and maintained through a combination of an inhalational agent and intravenous medications. The inhalational agent used was either sevoflurane or desflurane at the preference of the anesthesiologist. The concentration of the inhalational agent was maintained at minimum alveolar concentration, defined as the concentration of inhaled anesthetic at which 50% of patients do not move in response to a surgical stimulus. The intravenous agents were used in various combinations of propofol (dosing range from 50-100 μg/kg/min), remifentanil (dosing range from 0.02-0.05

μg/kg/min) and dexmedetomidine (dosing range from 0.1-0.3 μg/kg/hr). The anesthesia regime was titrated to clinical effect, and hemodynamic parameters were based on the patient's baseline preoperative vital signs. For each patient, a supraglottic airway device was placed to maintain a patent airway and ensure the delivery of oxygen. A muscle relaxant (rocuronium, dosing range from 50-100 mg) was used to facilitate airway device placement.

Furthermore, to help with intraoperative and postoperative analgesia, a regional anesthesia technique was also employed to anesthetize the skin, subcutaneous tissue, muscle, and periosteum layers of the scalp and cranium. Superficial nerves innervating these structures were anesthetized by infiltrating local anesthesia (ropivacaine 0.5% with epinephrine 1:200,000, 1-3 cc volume of injection at each site) around the nerves to provide analgesia lasting for about 8-12 hours. Once the dura was opened, CS delineation with SSEPs was conducted in the anesthetized state and recorded with the high-density ECoG grid placed on the presumed location of the hand knob. The patient then emerged from general anesthesia by discontinuing all the anesthesia agents. The airway device was removed when the patient could spontaneously ventilate, follow simple commands, and was hemodynamically stable. The time from discontinuing the anesthetics to removing the airway device ranged from 10 to 20 minutes. After removing the airway device, patients still needed a few minutes of focused direction and guidance to be fully awake and aware of the operative surroundings. This was accomplished by frequently asking the patient to follow simple commands and orienting them to the environment. When the response was prompt and regular, the patient was deemed ready to begin neurological testing using SSEPs in the awake state. Once the SSEPs were assessed in the anesthetized and awake state and tumor resection was complete, the patient was then administered general anesthesia again until the completion of surgery.

2.3 SSEP Protocol

In each patient, the primary location of the tumor was in the vicinity of the sensorimotor area, as indicated in Table 1. For each patient, the neurosurgeon placed the subdural ECoG electrode grid on the convexity over the presumed location of the CS and cortical hand knob for the median nerve stimulation assessment. A schematic description of this setup is illustrated in Figure 1A-C. For patients 1-4, we used a 25-53 channel hybrid grid (CorTec GmbH, Freiburg Germany) with 10mm contact spacing and 1-2.7 mm contact diameter. For patients 5-6, we used a 64-channel

(8x8) high-density subdural grid, whereas, for patients 7-8, we used a 32-channel high-density grid (Ad-Tech Medical Instrument Co., WI, USA) with 5mm contact spacing and 2mm contact diameter. A 1x4 electrode strip was flipped and placed under the dura as reference and ground. Two disposable conductive solid-gel electrodes were attached over the skin at the wrist such that the contralateral median nerve could be stimulated (Figure 1A). Using the Food and Drug Administration-approved clinical 2 or 4 channels EMG/EP Measuring System (Neuropack S1 MEB-9400), we stimulated the median nerve at a frequency of 0.6Hz with a bipolar square wave electric pulse of 200 μs (Figure 1A) and a current intensity increased from 5 to 15mA until small twitches of their thumb abductor pollicis brevis were observed as recommended in the standard protocol of the American Clinical Neurophysiology Society (ACNS 2015). SSEPs were recorded while the patient was under anesthesia and after the patient was fully awake. In each state, over 150 median nerve stimulation trials were delivered for reproducible cortical SSEP responses to be identified. We recorded bipolar forearm electromyography (EMG) during the median nerve stimulation to capture the stimulation pulses, which appeared in the form of sharp spikes (S; Figure 1C, bottom). The neural data from the ECoG grids and bipolar surface EMG from the forearm were recorded with a multichannel bio-signal amplifier (gHIamp: 256 channels, g.tec medical engineering GmbH, Graz Austria) at a sampling frequency of 2.4KHz and 24bit A/D resolution. All behavioral and neural data were acquired, synchronized, and visualized in real-time intraoperatively using Simulink/MATLAB (MathWorks, Natick, MA, USA) and gHIsys block sets (g.tec medical engineering GmbH, Graz Austria).

2.4 Electrode selection and co-registration on the individual 3D MRI for CS and sensorimotor identification

Thin-sliced preoperative magnetic resonance imaging (MRI) scans, based on a Fluid Attenuated Inversion Recovery (FLAIR) sequence (Ashikaga et al. 1997) (repetition time of 6.8s, echo time of 101.6ms, slice thickness of 1mm with 262,144 pixels), were obtained for each patient and were used to generate a 3D cortical mesh with Statistical Parametric Mapping (SPM12) (Ashburner et al. 2014). Using an in-house developed electrode registration software (Jiang et al. 2017) and a pipeline from our previous studies (Asman et al. 2021), we co-registered the 3D brain mesh with electrodes whose locations were determined based on anatomical landmarks, such as the cortical hand knob, central sulcus, and blood vessels, viewed from intraoperative images

(Figure 1B and Supplementary material Figures S1). The CS and the primary somatosensory (S1) and motor (M1) area borders were retrospectively identified on the 3D mesh by two neurosurgeons blinded to the electrophysiology data, with sample positions from the intraoperative neuronavigation and photos. The electrodes within the S1 and M1 borders were labeled accordingly and selected for further analysis.

2.5 Spectral analysis and power estimation

All ECoG recordings were visually examined to remove corrupted channels and artifacts. The neural data were processed offline using MATLAB 2018b (MathWorks, Natick, MA, USA). The ECoG trace was filtered with a high-pass filter from 30Hz to minimize baseline fluctuations as recommended by the ACNS (ACNS 2015). To estimate the SSEP, we aligned the ECoG traces to the stimulation pulse onset (S) in Figure 1C and then averaged across trials in individual channels. The averaged trace revealed the posterior N20 and anterior P20 peaks between +17 and +25 ms (Figure 1D). The spectral features were evaluated from the same ECoG traces that we aligned to the stimulation onset. Each epoch containing data from -150 to +250 ms relative to the stimulation pulse onset was represented in the time-frequency domain using Stockwell transform (Stockwell et al. 1996). Stockwell transform relies on a frequency-dependent Gaussian window width, which results in a nonuniform time-frequency resolution. After averaging the time-frequency maps, we normalized the spectrogram through element-wise division along the frequency dimension using a baseline power of -150 to 0 ms before stimulation onset. We transformed the averaged spectrograms into a decibel (dB) scale to yield the centered spectrograms. The time-frequency maps were visible for frequencies up to 900Hz (Figure 1E). To assess the average spectral modulations in each cortical region and state, we averaged the time-frequency maps across S1 and M1 channels separately in the anesthetized and awake states.

To assess the temporal power modulations for each patient in each state, we filtered the epochs using an FIR bandpass filter (Barlett-Hanning window, 51 tap filter) in the gamma range (60-250Hz; Figure 1F). We then computed the Hilbert transform (Benitez et al. 2001) to retrieve the magnitude envelope from the filtered epoch. We then squared the envelope to compute the temporal power trace and normalized it against the respective baseline preceding the stimulation onset.

2.6 Spatial patterns of the N20 and spatial spectral patterns of gamma

The amplitude distribution of the SSEP at N20 was visualized on a 2D grid as a heatmap using in-house designed visualization software (Jiang et al. 2017), similar to our earlier study (Asman et al. 2021). We compared the spatial features of the N20 to that of the spatial-spectral non-phase locked components between +50 to +250ms. The spatial matrices obtained from each channel's power ratio in the gamma range were interpolated by performing Delaunay triangulation (Lee et al. 1980, Jiang et al. 2018, Jiang et al. 2020) on the registered electrode positions and visualized on the individual MRI rendering and 2D grid (Figures 1G). The site showing the strongest sub-band power was identified in each state to determine its spatial relation relative to the peri-Rolandic cortex.

2.7 Statistical Analysis

The discrimination between S1 and M1 was assessed based on the gamma power and the peak amplitude at N20. We used the area under the curve (AUC) of the receiver operating characteristic (ROC) curve to determine the accuracy in distinguishing the somatosensory channels from the motor channels. The statistical significance of gamma power in each consciousness state for M1 and S1 channels was tested using Student's t-test with a significance threshold p-value of 0.05. Paired t-tests were used to compare the gamma oscillations between the anesthetized and awake states. In addition, we estimated the spatial correlation between the SSEPs amplitude at N20 and the spectral power in the gamma range using the Pearson correlation coefficient.

3. Results

On average, 126 ± 47 (mean ± SD) artifact-free stimulation trials were recorded in the anesthetized state, and 106 ± 49 stimulation trials were recorded in the awake state from 8 patients (P1 to P8). The number of trials recorded in each state was not significantly different across patients (paired t-test, t (7) =1.1584, p=0.2847). Below, we present the findings relative to the spatial topography of the SSEP N20 peak and the spatio-spectral patterns in the gamma range.

3.1 Spatial Characteristics of SSEP Amplitude and Spectral Modulations

The spatial topography of SSEP peak amplitude at N20 and late gamma spectral modulation are shown in Figure 2. Consistent with our earlier study (Asman et al., 2021), the spatial

topography of SSEP N20 in the anesthetized and awake states delineated the CS and distinctly divided the somatosensory and motor areas (Figure 2A and 2C) for P1, P2, P4-P7. For P3, the ECoG grid did not cross the CS; therefore, there was no phase reversal, and only blue patches could be seen from the heat map. However, while the grid traversed CS for P8, the SSEPs were misleading in the anesthetized state since the spatial heat map did not correlate with the CS and sensorimotor borders (Figure 2C, bottom). We observed blue patches in M1 and S1, while green to red patches were seen in more posterior regions. The blue patches showed stronger intensities in S1. In the awake state for P8, no phase reversal was observed, and the SSEP heat map showed only blue patches with stronger intensities in the somatosensory area. We also noted that channels with the maximum N20 peak amplitude (triangular symbol) were either the same or in proximity in the anesthetized and awake states. These channels were also associated with late gamma modulation (Figure 2B and 2D).

The spatial-spectral analysis revealed late gamma activity (red patches) for all patients in the awake state that was very focal and predominant on channels near the CS and S1 (Figures 2A and D). In contrast, we saw late gamma suppression (blue patches) in the anesthetized state in S1 in several subjects. Even though the SSEP was misleading for P8, we observed late gamma suppression in the anesthetized state and late gamma increase in the awake state, primarily in S1. P1 and P3 also had late gamma power increase at channels near the CS in the anesthetized state, along with suppressions in the S1.

We assessed the similarity in spatial topography of the SSEP amplitude at N20 and late gamma activities by performing a correlation analysis across the S1 and M1 channels in the awake and the anesthetized states. The results of this analysis are shown in Figure 3. In Figure 3A, the spatial correlation for the SSEP amplitude at N20 between states was high and consistently positive across patients. The spatial correlation for the late gamma power between states was inconsistent across patients (Figure 3A). We further assessed the spatial correlation between the N20 and the late gamma in Figure 3B, which was inconsistent in the anesthetized state across patients. While in the awake state, the spatial correlation was consistently negative (Figure 3B).

3.2 Accuracy of M1 vs. S1 discrimination

In Figure 4, we show the power levels for the late gamma bands in the M1 and S1 regions and the AUC distribution regarding the discrimination between somatosensory and motor areas using

either the gamma power level or the peak amplitude at N20. Since the ECoG grid for P3 did not cross the CS anteriorly, this subject was excluded from this analysis. In Figure 4A, we can see that the late gamma suppression was not significantly different between S1 and M1 in the anesthetized state (paired t-test t (6) = -1.2499, p = 0.2579). In contrast, in the awake state, the late gamma power increase was significantly greater in S1 than in M1 (paired t-test t (6) = 4.7165, p<0.01). The accuracy of discrimination between the primary somatosensory and motor areas using the SSEPs N20 and late gamma activities was quantified with the area under the ROC (AUC). This is illustrated for P5 in Figure 4B. The overall accuracy for each patient in each state for the N20 and late gamma bands is shown in Figure 4C. Table 2 shows the statistical results contrasting the accuracy for each band and state. Overall, we noted that the M1 and S1 discrimination was high in each state with N20. In contrast, there was a higher accuracy of discrimination in the awake state than in the anesthetized state for the late gamma. The N20 showed higher discrimination accuracy than the late gamma in the anesthetized state (see table 2), whilst in the awake state, their levels of discrimination were not significantly different. We further assessed the discrimination accuracy with the SSEPs' high-frequency oscillations (450-700Hz, HFO) and early gamma activity (60-250Hz) within the first 50ms after stimulation onset. Details of this analysis are shown in the Supplementary material Section S2 and Figure S2.

3.3 State-specific characteristics of induced modulations

Figure 5A shows the stimulus-aligned baseline normalized group average time-frequency maps for S1 and M1 channels in the awake and anesthetized states. The temporal profile power change in the gamma (60-250Hz) band concerning baseline is shown in Figure 5B. We noted substantial differences in late gamma activity between anesthetized and awake states in M1 and S1. Specifically, the late gamma modulation was temporarily isolated, occurring from +50ms to +250ms in M1 and S1 and was more prominent in S1 in the awake state than in any other case. Interestingly, the late gamma activity was suppressed in the anesthetized state in both M1 (independent t-test t (6) = -3.4625, p = 0.0134) and S1 (independent t-test t (7) = -2.6301, p = 0.0339), as can be seen in Figure 5A and Figure 5B (blue line). In contrast, in the awake state, the late gamma power increased significantly relative to baseline both in M1 (independent t-test t (6) = 4.7552, p < 0.01) and S1 (independent t-test t (7) = 4.5791, p < 0.01; Figure 5A and Figure 5B, red line). Furthermore, the difference in late gamma power between the anesthetized and the awake

state was highly significant for M1 (ΔdB: 3.33 dB ± 0.06 dB; paired t-test t (6) = -5.5651, $p < 0.01$) and for S1 (ΔdB: 7.73dB ± 1.33 dB; paired t-test t (7) = -5.1402, $p < 0.01$; Figure 5C). More specifically, the increase in gamma power from anesthetized to awake state was consistent across all subjects in S1 and M1, although with a larger difference in S1 (Figure 5C). We also observed a consistent difference in power between states for the SSEP's HFO but an inconsistent difference for the early gamma activity (see Supplementary material Section S3 and Figure S3).

We further assessed the alterations in the amplitude of N20/P20 between the anesthetized and awake states in M1 and S1. While we observed subtle differences in peak amplitude between states in Figure 2C, the difference in S1 and M1 between states was not significant (S1: paired t-test t (6) = -0.2563, p = 0.8063; M1: paired t-test t (5) = 0.3296, p=0.7551).

4. Discussion

We assessed the spectral modulations in the peri-Rolandic cortex induced by median nerve stimulation and the effect of anesthesia on these spectral features. We found that the intraoperative sensorimotor mapping does not need to be limited to only SSEP phase reversal. Indeed, the induced late latency gamma-band modulation extending beyond 50ms following the stimulation onset has the potential to accurately localize the primary somatosensory area and predict the state of consciousness of the patients even when the SSEP phase reversal method is not conclusive.

4.1 Correlation of peak temporal and spectral activities to Rolandic cortex

The examination of the amplitude maps of the SSEPs at N20 in Figures 2A and C showed a clear delineation of the CS (except for P8), as found also in our previous study (Asman et al. 2021) in each state. However, we observed no significant difference in N20/P20 amplitude between consciousness states. Some studies have shown that general anesthesia causes amplitude depression in SSEPs (Burnos et al. 2016, Kalkman et al. 1992, Boisseau et al. 2002), while others have shown a minimal to no effect on cortical SSEP amplitude (Hasan et al. 2018, Tobias et al. 2008, Bala et al. 2005, Sturaitis et al. 2003). It is possible that different anesthesia regimens have different effects on the N20/P20 amplitude, which needs to be further studied.

The late gamma power increase in the awake state vividly outlined S1 consistently in all patients (Figure 2D) and was more prominent in S1 than in M1 (Figure 5A). In the awake state, the gamma power showed a high level of discrimination between somatosensory and motor areas

with accuracy, like the N20. In contrast, the late gamma suppression in the anesthetized state was more pronounced in S1 in some patients (Figure 2D, P4, and P5) and M1 in others (Figure 2D, P2, and P6) and showed weak discrimination between somatosensory and motor areas.

The late gamma activity was associated with a noticeable change in Its spatial profile from the anesthetized to the conscious state. We also observed a moderate and consistent spatial correlation between the late gamma and the N20 amplitude in the awake state but not in the anesthetized state (Figures 3B). These results suggest that gamma modulation changed not only in power level but also in spatial characteristics with the transition from the anesthetized to the conscious state.

P8 SSEPs in the anesthetized state failed to provide a delineation of the CS (see Figure 2C). Here the SSEP phase reversal and heatmap were unreliable since they did not correlate with the sensorimotor borders. In all patients except P8, the SSEPs heatmap showed a characteristic gradient where the heatmap decreased in intensity further away from the CS. This was more pronounced in the posterior regions, where the intensity of the heat map was high near the CS and lowered as we moved further away from the CS in the posterior direction, with the contrasting color in the anterior regions. However, for P8, this gradient was observed from the posterior to the anterior areas with the contrasting color in the more posterior regions. While the SSEPs were misleading for P8, the presence of the late gamma suppression in the anesthetized state hinted at the location of the primary somatosensory area. In the awake state, although strong activities could be seen in S1 (see Figure 2C) from the SSEP heat map in P8, no clear phase reversal was observed for proper CS delineation. Yet, the late increase in gamma activity (characteristic to S1)provided clear discrimination between M1 and S1, solidifying its significance in delineating the CS.

4.3 Significance of early and late gamma

During the presurgical mapping of the sensorimotor cortex, an increase in gamma oscillations has often been used as a marker of cortical activation associated with somatosensory or motor tasks (Miller et al., 2007, Schalk et al., 2008). Studies have shown that early induced gamma oscillations in SSEPs are based on the initial cortical response to the electrical stimuli which emerge in the postcentral gyrus. These early gamma oscillations gradually decrease in frequency range and show no significant difference between anesthetized and awake states (Kisley et al., 2006, Schubert et al., 2006, Fukuda et al., 2008, 2010). Fukuda et al. demonstrated that the gamma augmentation (30–100 Hz maximally at 25 ms on average) gradually slowed down in frequency

and evolved into beta augmentation (14–28 Hz; maximally at 42 ms on average) and alpha augmentation (8–12 Hz; maximally at 97 ms on average) (Fukuda et al. 2008, 2010). Since we assessed the spectral modulations after high-pass filtering at 30Hz, we did not observe any alpha-beta activity. While we noted the early evoked gamma response, consistent with previous findings, occurring up to 50ms and which showed no difference between states (see Figure 5A and Supplementary material Figure S3C), the low-rate median nerve stimulations at 0.6Hz allowed us to record and analyze cortical oscillatory activity extending beyond 50ms. Other studies have observed a phasic response up to 50ms in S1 and a tonic response up to 250ms in the perisylvian regions following low rate (1Hz) stimulation to the median nerve (Fisch et al. 2009, Avanzini et al. 2016, Del Vecchio et al. 2019).

We found two temporally distinct gamma components in response to median nerve stimulation (Figure 5B) in M1 and S1. The early component (15-35ms) occurred in both the anesthetized and awake states (Supplementary material Figure S3). The late component was more temporally widespread (50-250ms), suppressed in the anesthetized state, and enhanced in the awake state (Figure 2A, B, and E and Figure 5A and B)., Numerous studies have reported that a consciously perceived external stimulus resulted in neural responses that comprise an early event-related component accompanied by a late sustained one (Sergent et al. 2005, Fisch et al., 2009, Avanzini et al., 2016). Authors have surmised that the critical correlate of conscious access was associated with the late neural response (Sergent et al., 2005, Fisch et al., 2009, Avanzini et al., 2016). In this study, we observed late gamma oscillations only in the awake state that were more pronounced in S1 than in M1 and lasted up to 250ms (Figure 5 A and B). MEG studies have shown that event-related high gamma (60-90Hz) power increase in the somatosensory cortex was prolonged by tactile attention from 100ms to 500ms (Bauer et al. 2006). Ray et al. found that significant gamma responses (60–150 Hz) occurring in the somatosensory area at longer latencies (300-800ms) were enhanced when the respective tactile stimuli were attended (Ray et al. 2008). Since, in this study, the patients in the awake state were aware of the electrical stimulation and were asked to pay attention to their thumb twitching, it is quite possible that the increase in late gamma activity was associated with the conscious processing of the somatosensory sensations induced by median nerve stimulation.

We observed a late gamma power suppression in the anesthetized state both in S1 and M1 (Figure 5A, B, and D). Sloan et al. indicated that anesthetics block or depress the cortical

somatosensory responses by enhancing the inhibitory effect of gamma-aminobutyric acid (GABA) and blocking the excitatory effect of glutamate (Sloan et al. 2002a, 2002b). As the anesthetic drug effect increases, there is a gradual slowing of the frequency and a reduction in amplitude and power of the electroencephalograph (Sloan et al. 2002b). Consistently, the inhibitory nature of isoflurane anesthesia has been considered to play a low-pass filtering role in spike transmission at central excitatory synapses (Wang et al., 2020). Since we noted a significant decrease in late gamma power in the anesthetized state, we hypothesize that the gamma suppression was due to the impact of the anesthetics facilitating the effect of the complex inhibitory mechanisms mediated by GABA-modulated connectivity within the sensorimotor cortex and blocking the excitatory effects of glutamatergic synapses.

4.4 Practical Implication and Reproducibility

Using a pipeline that was implemented and described in our previous study (Jiang et al., 2018), the SPM12 (Kiebel et al., 1997), a free and commonly used open-source software, was employed to create a segmented volume of the gray and white matter from each patient's preoperative thin slice MRI, where it was rendered in MATLAB to create a 3D cortical mesh of the brain (see Supplementary material Section S1 and Figure S1). The in-house electrode co-registration software consists of a MATLAB graphical user interface (GUI) that integrates MATLAB functions for the 3D visualization and electrode coregistration. The software library is freely available on GitHub at https://github.com/InceLab/BrainMap with a sample data set.

In order to guide surgical planning in a clinical setting, we also developed a real-time system for identifying focal gamma modulation in S1 and visualizing the extracted pattern over a 2D plane intraoperatively (Asman et al., 2022). The data acquisition and signal processing system were implemented in MATLAB Simulink using g.Hisys Simulink Libraries (Simulink Highspeed Library v3.16.01, g.Tec, Graz, Austria) and MATLAB digital signal processing Toolbox (MathWorks, Natick, MA, USA). A heat map is generated in real-time in the operating room in a short time to assist with the delineation of CS or identification of sensorimotor area during awake craniotomies (see Supplementary material section 4 for detailed description and demonstrations in Videos 1 and 2).

5. Conclusions

The spatial distribution of the SSEPs spectral features recorded using high-density ECoG grids reliably defined the contours of the CS even when the N20 phase reversal failed. In particular, the late gamma modulation was localized in S1. In addition, the late gamma difference in the sensorimotor area between the anesthetized and awake states was significant, which can easily be detected during a real-time awake craniotomy. Therefore, the median nerve stimulation-induced late gamma modulation can potentially serve as a neurobiomarker to define the sensorimotor area and monitor the state of consciousness in patients undergoing awake craniotomy.

Supplementary Material

Supplementary_Material_HFO_EarlyGamma.pdf

Video_1_SSEP_RealTime_Map.mp4

Video_2_SSEP_Gamma_RealTime_Map.mp4

Reference

Allison TR, McCarthy GR, Wood CC, Darcey TM, Spencer DD, Williamson PD. Human cortical potentials evoked by stimulation of the median nerve. II. Cytoarchitectonic areas generating short-latency activity. J. Neurophysiol. 1989;62(3):694-710. https://doi.org/10.1152/jn.1989.62.3.694

American Clinical Neurophysiology Society. Guideline 11B: Recommended standards for intraoperative monitoring of somatosensory evoked potentials. 2009. Retrieved from ACNS. org. 2015. https://doi.org/10.1080/21646821.2016.1245527

Ashburner, J., Barnes, G., Chen, C.C., Daunizeau, J., Flandin, G., Friston, K., Kiebel, S., Kilner, J., Litvak, V., Moran, R. and Penny, W. SPM12 manual. WTCN., London, UK, 2464, p.4.; 2014

Ashikaga R, Araki Y, Ishida O. MRI of head injury using FLAIR. Neuroradiology. 1997;39(4):239-42. https://doi.org/10.1007/s002340050401

Asman P, Prabhu S, Bastos D, Tummala S, Bhavsar S, McHugh TM, Ince NF. Unsupervised machine learning can delineate the central sulcus by using the spatiotemporal characteristic of somatosensory evoked potentials. J. Neural Eng. 2021;18(4):046038. http://dx.doi.org/10.1088/1741-2552/abf68a

Asman P., Prabhu S., Tummala S, and Ince NF. Real-time delineation of the central sulcus with the spatial profile of SSEPs captured with a high-density ECoG grid. 44th EMBC 2022 Jul 11 (pp. 4892-4895). IEEE. DOI: 10.1109/EMBC48229.2022.9871900

Avanzini P, Abdollahi RO, Sartori I, Caruana F, Pelliccia V, Casaceli G, Mai R, Lo Russo G, Rizzolatti G, Orban GA. Four-dimensional maps of the human somatosensory system. Proc. Natl. Acad. Sci. 2016. 113(13): E1936–E1943. https://doi.org/10.1073/pnas.1601889113

Avanzini P, Pelliccia V, Lo Russo G, Orban GA, Rizzolatti G. Multiple time courses of somatosensory responses in human cortex. Neuroimage. 2018; 169:22-226. https://doi.org/10.1016/j.neuroimage.2017.12.037

Bala E, Sessler DI, Nair DR, McLain R, Dalton JE, Farag E. Motor and somatosensory evoked potentials are well maintained in patients given dexmedetomidine during spine surgery. Anesthesiology. 2008;109(3):417-25. https://doi.org/10.1097/ALN.0b013e318182a467

Banoub M, Tetzlaff JE, Schubert A. Pharmacologic and physiologic influences affecting sensory evoked potentials: implications for perioperative monitoring. ASA. 2003;99(3):716-37. https://doi.org/10.1097/00000542-200309000-00029

Bauer M, Oostenveld R, Peeters M, Fries P. Tactile spatial attention enhances gamma-band activity in somatosensory cortex and reduces low-frequency activity in parieto-occipital areas. J. Neurosci. 2006;26(2):490-501. https://doi.org/10.1523/JNEUROSCI.5228-04.2006

Benitez D, Gaydecki PA, Zaidi A, Fitzpatrick AP. The use of the Hilbert transforms in ECG signal analysis. Comput. Biol. Med. 2001;31(5):399-406. https://doi.org/10.1016/S0010-4825(01)00009-9

Boisseau N, Madany M, Staccini P, Armando G, Martin F, Grimaud D, Raucoules-Aimé M. Comparison of the effects of sevoflurane and propofol on cortical somatosensory evoked potentials. Brit. J. Anaesth. 2002;88(6):785-9. https://doi.org/10.1093/bja/88.6.785

Burnos S, Fedele T, Schmid O, Krayenbühl N, Sarnthein J. Detectability of the somatosensory evoked high frequency oscillation (HFO) co-recorded by scalp EEG and ECoG under propofol. NeuroImage Clin. 2016; 10:318-25. https://doi.org/10.1016/j.nicl.2015.11.018

Cedzich C, Taniguchi M, Schäfer S, Schramm J. Somatosensory evoked potential phase reversal and direct motor cortex stimulation during surgery in and around the central region. Neurosurgery. 1996;38(5):962-70. DOI: 10.1097/00006123-199605000-00023

Del Vecchio M, Caruana F, Sartori I. Ipsilateral somatosensory responses in humans. The tonic activity of SII and posterior insular cortex. Brain Struct Funct. 2019;224(1):9-18. https://doi.org/10.1007/s00429-018-1754-6

Duffau H, Lopes M, Arthuis F, Bitar A, Sichez JP, Van Effenterre R, Capelle L. Contribution of intraoperative electrical stimulations in surgery of low-grade gliomas: a comparative study between two series without (1985–96) and with (1996–2003) functional mapping in the same institution. J. Neurol. Neurosurg. Psychiatry. 2005;76(6):845-51. http://dx.doi.org/10.1136/jnnp.2004.048520

Endisch C, Storm C, Ploner CJ, Leithner C. Amplitudes of SSEP and outcome in cardiac arrest survivors: a prospective cohort study. Neurology. 2015;85(20):1752-60. DOI: 10.1212/WNL.0000000000002123

Endisch C, Storm C, Ploner CJ, Leithner C. Amplitudes of SSEP and outcome in cardiac arrest survivors: a prospective cohort study. Neurology. 2015;85(20):1752-60. DOI: https://doi.org/10.1212/WNL.0000000000002123

Fisch L, Privman E, Ramot M, Harel M, Nir Y, Kipervasser S. Neural "ignition": enhanced activation linked to perceptual awareness in human ventral stream visual cortex. Neuron. 2009. 65(4);562-574. https://doi.org/10.1016/j.neuron.2009.11.001

Friedman WA. Somatosensory evoked potentials in neurosurgery. Clin. Neurosurg. 1988. 34:187-238. DOI: 10.4103/0028-3886.66454

Fukuda M, Juhász C, Hoechstetter K, Sood S, Asano E. Somatosensory-related gamma-, beta- and alpha-augmentation precedes alpha-and beta-attenuation in humans. Clin. Neurophysiol. 2010;121(3):366-75. https://doi.org/10.1016/j.clinph.2009.10.036

Fukuda M, Nishida M, Juhasz C, Muzik O, Sood S, Chugani HT, Asano E. Short-latency median-nerve somatosensory-evoked potentials and induced gamma-oscillations in humans. Brain. 2008;131(7):1793-805. https://doi.org/10.1093/brain/awn100

Gobbelé R, Waberski TD, Simon H, Peters E, Klostermann F, Curio G, Buchner H. Different origins of low-and high-frequency components (600 Hz) of human somatosensory evoked potentials. Clin. Neurophysiol. 2004;115(4):927-37. https://doi.org/10.1016/j.clinph.2003.11.009

Gross DW, Merlet I, Boling W, Gotman J. Relationships between the epileptic focus and hand area in central epilepsy: combining dipole models and anatomical landmarks. J. Neurosurg. 2000;92(5):785-792. https://doi.org/10.3171/jns.2000.92.5.0785

Hasan MS, Tan JK, Chan CY, Kwan MK, Karim FS, Goh KJ. Comparison between the effect of desflurane/remifentanil and propofol/remifentanil anesthesia on somatosensory evoked potential monitoring during scoliosis surgery—A randomized controlled trial. J. Orthop. Surg. 2018;26(3):2309499018789529. https://doi.org/10.1177/2309499018789529

Huncke, K., Van de Wiele, B., Fried, I. and Rubinstein, E.H. The asleep-awake-asleep anesthetic technique for intraoperative language mapping. Neurosurgery 1998, 42(6), pp.1312-1316. DOI: 10.1097/00006123-199806000-00069

Jiang T, Liu S, Pellizzer G, Aydoseli A, Karamursel S, Sabanci PA, Sencer A, Gurses C, Ince NF. Characterization of hand clenching in human sensorimotor cortex using high-, and ultra-high frequency band modulations of electrocorticogram. Front. Neurosci. 2018 27;12:110. https://doi.org/10.3389/fnins.2018.00110

Jiang T, Pellizzer G, Asman P, Bastos D, Bhavsar S, Tummala S, Prabhu S, Ince NF. Power modulations of ECOG alpha/beta and gamma bands correlate with time-derivative of force during hand grasp. Front. Neurosci. 2020;14:100. DOI: 10.3389/fnins.2020.00100

Jiang T, Siddiqui H, Ray S, Asman P, Ozturk M, Ince NF. A portable platform to collect and review behavioral data simultaneously with neurophysiological signals. 39th EMBC 2017; (pp. 1784-1787). https://doi.org/10.3389/fnins.2020.00100

Kalkman C, Drummond J, Patel P, Sano T, Chesnut R. Effects of droperidol, pentobarbital and ketamine on myogenic transcranial motor evoked responses in humans. Anesthesiology. 1992;77(3A). DOI: 10.1227/00006123-199412000-00008

Kiebel, S. J., Ashburner, J., Poline, J. B., and Friston, K. J. (1997). MRI and PET coregistration–a cross-validation of statistical parametric mapping and automated image registration. NeuroImage 5, 271–279. doi: 10.1006/nimg.1997.0265

Kisley MA, Cornwell ZM. Gamma and beta neural activity evoked during a sensory gating paradigm: effects of auditory, somatosensory, and cross-modal stimulation. Clin. Neurophysiol. 2006;117(11):2549-63. https://doi.org/10.1016/j.clinph.2006.08.003

Kombos T, Suess O, Ciklatekerlio Ö, Brock M. Monitoring of intraoperative motor evoked potentials to increase the safety of surgery in and around the motor cortex. J. Neurosurg. 2001;95(4):608-14. https://doi.org/10.3171/jns.2001.95.4.0608

Lavrador JP, Ghimire P, Brogna C, Furlanetti L, Patel S, Gullan R, Ashkan K, Bhangoo R, Vergani F. Pre-and intraoperative mapping for tumors in the primary motor cortex: decision-making process in surgical resection. J. Neurol. Surg. A Cent. Eur. Neurosurg. . 2021;82(04):333-43. DOI: 10.1055/s-0040-1709729

Lee DT, Schachter BJ. Two algorithms for constructing a Delaunay triangulation. Int. J. Comput. Inf. Sci. 1980;9(3):219-42. https://doi.org/10.1007/BF00977785

Miller KJ, Shenoy P, Miller JW, Rao RP, Ojemann JG. Real-time functional brain mapping using electrocorticography. Neuroimage. 2007;37(2):504-7. DOI: 10.1016/j.neuroimage.2007.05.029

Nuwer MR. Localization of motor cortex with median nerve somatosensory evoked potentials. Intraoperative neurophysiologic monitoring in neurosurgery. Neuroimage. 2007.05.029 Springer, Berlin, Heidelberg. 1991; 63-71. https://doi.org/10.1016/j.

Oh SH, Park KN, Choi SP, Oh JS, Kim HJ, Youn CS, Kim SH, Chang K, Kim SH. Beyond dichotomy: patterns and amplitudes of SSEPs and neurological outcomes after cardiac arrest. Crit. Care. 2019(1):1-11. https://doi.org/10.1186/s13054-019-2510-x

Pondal-Sordo M, Diosy D, Téllez-Zenteno JF, Girvin JP, Wiebe S. Epilepsy surgery involving the sensory-motor cortex. Brain. 2006;129(12):3307-14. https://doi.org/10.1093/brain/awl305

Ray S, Niebur E, Hsiao SS, Sinai A, Crone NE. High-frequency gamma activity (80–150 Hz) is increased in the human cortex during selective attention. Clin. Neurophysiol. 2008;119(1):116-33. https://doi.org/10.1016/j.clinph.2007.09.136

Schalk G, Miller KJ, Anderson NR, Wilson JA, Smyth MD, Ojemann JG, Moran DW, Wolpaw JR, Leuthardt EC. Two-dimensional movement control using electrocorticographic signals in humans. J. Neural Eng. 2008;5(1):75. http://dx.doi.org/10.1088/1741-2560/5/1/008

Schubert, R., Blankenburg, F., Lemm, S., Villringer, A. and Curio, G. Now you feel it—now you don't: ERP correlates of somatosensory awareness. Psychophysiology. 2006, 43(1), pp.31-40. https://doi.org/10.1111/j.1469-8986.2006.00379.x

Sergent, C., Baillet, S. and Dehaene, S. Timing of the brain events underlying access to consciousness during the attentional blink. Nat. Neurosci. 2005 8(10), pp.1391-1400. https://doi.org/10.1038/nn1549

Sheth SA, Eckhardt CA, Walcott BP, Eskandar EN, Simon MV. Factors affecting successful localization of the central sulcus using the somatosensory evoked potential phase reversal technique. Neurosurgery. 2013;72(5):828-34. DOI: 10.1227/NEU.0b013e3182897447

Sloan TB, Heyer EJ. Anesthesia for intraoperative neurophysiologic monitoring of the spinal cord. Clin. Neurophysiol. Pract. 2002a;19(5):430-43. DOI: 10.1097/00004691-200210000-00006

Sloan TB. Anesthesia management and intraoperative electrophysiological monitoring. In: Koht A, Sloan T, Toleikis J (eds.) Monitoring the Nervous System for Anesthesiologists and Other Health Care Professionals, 2017 (pp. 317-341). Springer, Cham. DOI: 10.1007/978-3-319-46542-5_19

Sloan TB. Anesthetics and the brain. Anesthesiol. Clin. North Am. 2002b;20(2):265-92. https://doi.org/10.1016/S0889-8537(01)00002-5

Stockwell RG, Mansinha L, Lowe RP. Localization of the complex spectrum: the S transform. IEEE Trans. Signal Process. 1996;44(4):998-1001. DOI: 10.1109/78.492555

Sturaitis MK, Ford EW, Palac SM, Smith MC, Tuman KJ. Effect of dexmedetomidine on operative conditions and electrocorticographic responses during asleep craniotomy for seizure focus resection. Anesthesiology. 2003;99:A290.

Tobias JD, Goble TJ, Bates G, Anderson JT, Hoernschemeyer DG. Effects of dexmedetomidine on intraoperative motor and somatosensory evoked potential monitoring during spinal surgery in adolescents. Paediatr. Anaesth. 2008;18(11):1082-8. https://doi.org/10.1111/j.1460-9592.2008.02733.x

Wang HY, Eguchi K, Yamashita T, Takahashi T. Frequency-dependent block of excitatory neurotransmission by isoflurane via dual presynaptic mechanisms. J. Neurosci. 2020;40(21):4103-15. https://doi.org/10.1523/JNEUROSCI.2946-19.2020

Woolsey CN, Erickson TC, Gilson WE. Localization in somatic sensory and motor areas of the human cerebral cortex as determined by direct recording of evoked potentials and electrical stimulation. J. Neurosurg. 1979;51(4):476-506. https://doi.org/10.3171/jns.1979.51.4.0476

Tables

Table 1: Tumor location per patient

Patient	Hemisphere	Tumor Infiltration area
P1	Right	Motor and somatosensory
P2	Left	Motor and premotor
P3	Left	Motor and premotor
P4	Left	Motor and somatosensory
P5	Left	Somatosensory and parietal lobule
P6	Left	Motor and somatosensory
P7	Right	Supplementary Motor Area
P8	Right	Motor Area

Table 2: Somatosensory versus motor areas discrimination accuracy

	Anesthetized	Awake	p-value
Late gamma	0.70±0.20	0.92±0.10*	0.0115*
N20	**0.92±0.03**	0.92±0.08	0.0473
p-value	**0.0177**	0.4626	

*$0.01<p<0.05$, paired t-test between the anesthetized and awake state
Bold signifies $0.01<p<0.05$, paired t-test between late gamma and N20

Figure legends

Figure 1: Pipeline of Analysis: (A) Sketch of the stimulus-response pathway of the electrical stimulation comprising of a biphasic square wave with a pulse width of 200μs, at a current level up to 15A and a frequency of 0.6Hz applied to the contralateral median nerve. **(B)** Contralateral 3D cortical mesh obtained from patient 6 magnetic resonance imaging (MRI) with electrode co-registration based on the picture taken during the craniotomy. The central sulcus is marked with a red line on the brain, and the pink area is the image of the craniotomy taken in the OR and co-registered on the 3D image. (A: Anterior to CS, P: Posterior to CS, M: Medial, L: Lateral) **(C)** (top) Raw ECoG recording, viewed here for patient 6 in the awake state, from selected channels showing the time of electrical stimulation onset (S) (bottom) recorded from the bipolar EMG. **(D)** The broadband somatosensory evoked potential (SSEP) waveforms (>30Hz) aligned to stimulus onset and overlapped, shown for the first 50ms, where the N20 peak latency is marked (red). **(E)** Time-frequency map shown for Ch28 reveals the gamma (60-250Hz) oscillations up to 250ms. **(F)** The temporal profile of the gamma activity, up to 250ms. **(G)** The gamma spatial distribution is shown on the brain and grid (A: Anterior to CS, P: Posterior to CS). The black triangular dot on each grid locates the peak gamma activity. The central sulcus is marked with a gray line.

Figure 2: Cortical topography of N20 and late gamma activity to median nerve stimulation: (A) The 3D brain meshes display the electrode co-registration for P1 and P5, and the topography of N20, and late gamma activity in the anesthetized state and the awake state. Sites showing the maximum activity are marked with a black triangular symbol. (A: Anterior to CS, P: Posterior to CS, M: Medial, L: Lateral). **(B)** Time-frequency maps of channels with maximum N20, where we see gamma suppression in the anesthetized state and gamma power increase in the awake state from 60ms to 200 ms after median nerve stimulation. **(C)** The topography of N20 is shown for each patient in the anesthetized state and the awake state. **(D)** Topography for late gamma. The location of maximum activity is shown as a black triangular symbol. The dashed lines are the primary somatosensory (S1) and motor (M1) area border lines. The thick gray line is the central sulcus. The shaded region is the tumor infiltration area.

Figure 3: Spatial correlation of N20 amplitude and Spectral Power: (A) Scatter plot showing the spatial correlation between the anesthetized and awake state for somatosensory evoked potential (SSEP) amplitude at N20 (rho = 0.85 ± 0.19, mean ± SD), and gamma power (rho = 0.00 ± 0.64). **(B)** Scatter plot comparing the spatial correlation of the N20 amplitude and late gamma power between the awake and anesthetized state (An: rho =0.15±0.32, Aw: rho = -0.67 ± 0.19, paired t-test (6), $p < 0.01$, $t = -3.9583$).

Figure 4: Discrimination between S1 and M1. (A) Boxplot showing the change in power between the primary motor (M1) and somatosensory (S1) area in the anesthetized state and awake state for the gamma activity. A * above the data represents a t-test, where *:$0.01<p<0.05$ and, **: $p<0.01$, NS: non-significant. **(B)** The accuracy of discrimination between somatosensory and motor areas is shown as receiver operating characteristic (ROC) plots for P5 for (left) peak amplitude at N20 and (right) gamma power. Note: **(C)** The overall accuracy is estimated using the area under the curve (AUC) for (left) peak amplitude at N20 and (right) gamma power. A * between the data is the paired t-test, where *: $0.01<p<0.05$, **: $p<0.01$. NS: non-significant, An: Anesthetized, Aw: Awake

Figure 5: Spectral Assessment of Somatosensory Evoked Potential: (A) The average time-frequency map matrix showing the spectral modulation in the anesthetized and awake states in the primary somatosensory (S1) and motor (M1) regions. The dashed rectangle shows the late gamma modulation. **(B)** Group Gamma power modulation is shown for S1 and M1 compared between the awake and anesthetized states. **(C)** Scatter plot showing the level of change in gamma power in each patient from anesthetized to awake state for M1 and S1. A * above the data represents a paired t-test, where *: $0.01<p<0.05$, **: $p<0.01$, NS: non-significant, An: Anesthetized, Aw: Awake.

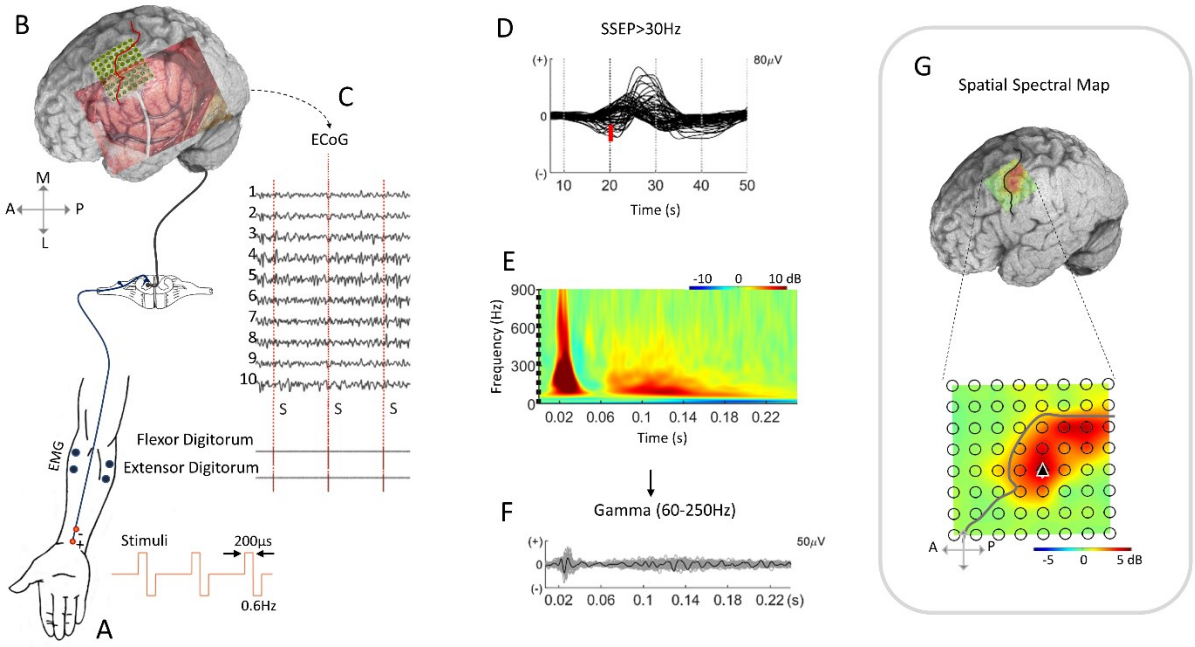
B
C
ECoG
M
A
P
L
1
2
3
4
5
6
7
8
9
10
S
S
S
EMG
Flexor Digitorum
Extensor Digitorum
Stimuli
200µs
0.6Hz
A
D
SSEP>30Hz
80µV
(+)
0
(-)
10
20
30
40
50
Time (s)
E
-10
0
10 dB
900
600
300
0
Frequency (Hz)
0.02
0.06
0.1
0.14
0.18
0.22
Time (s)
F
Gamma (60-250Hz)
50µV
(+)
0
(-)
0.02
0.06
0.1
0.14
0.18
0.22 (s)
G
Spatial Spectral Map
A
P
-5
0
5 dB

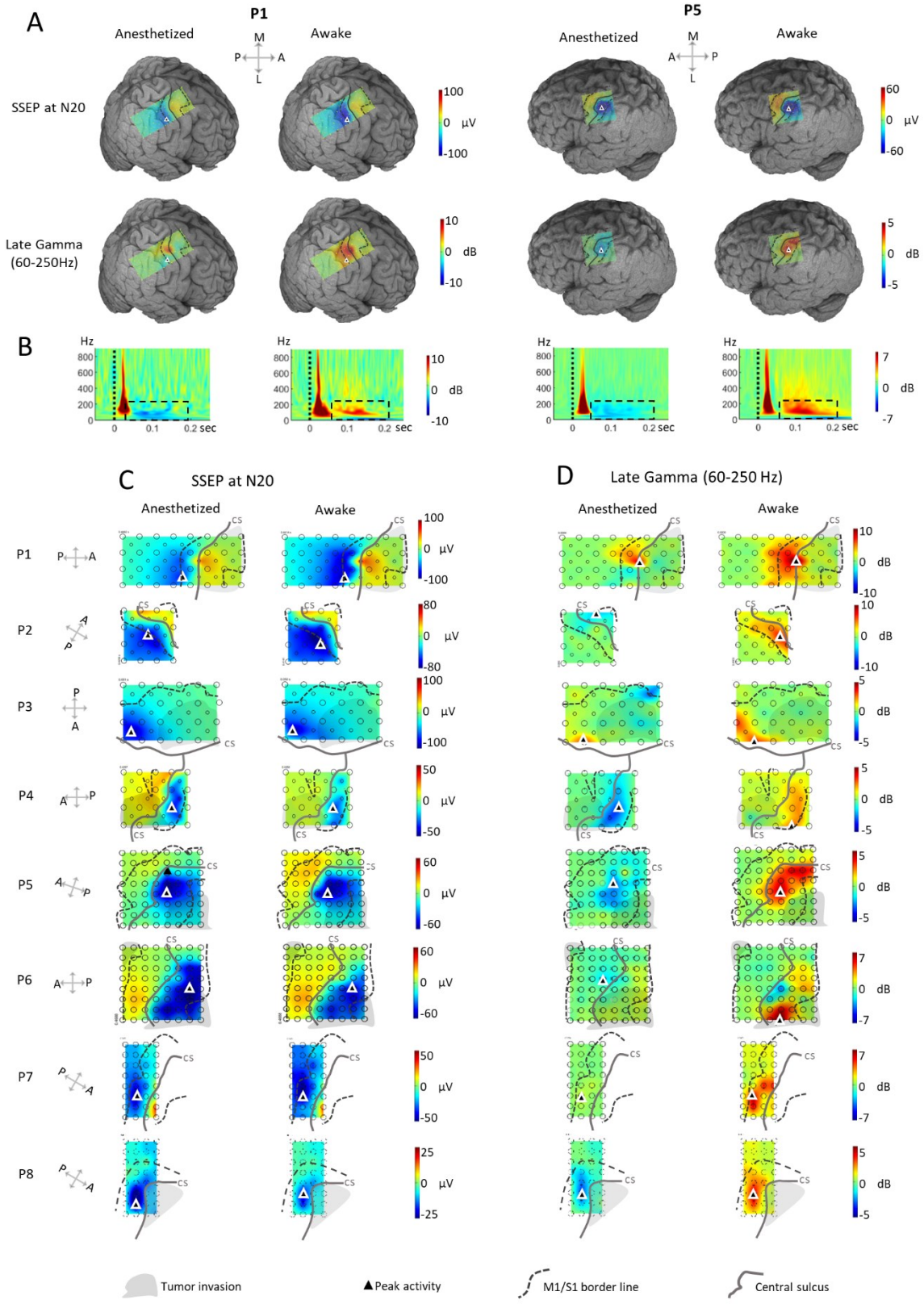
A
P1
P5
Anesthetized
Awake
SSEP at N20
Late Gamma (60-250Hz)
B
Hz
sec
C
SSEP at N20
D
Late Gamma (60-250 Hz)
P1
P2
P3
P4
P5
P6
P7
P8
CS
μV
dB
Tumor invasion
Peak activity
M1/S1 border line
Central sulcus

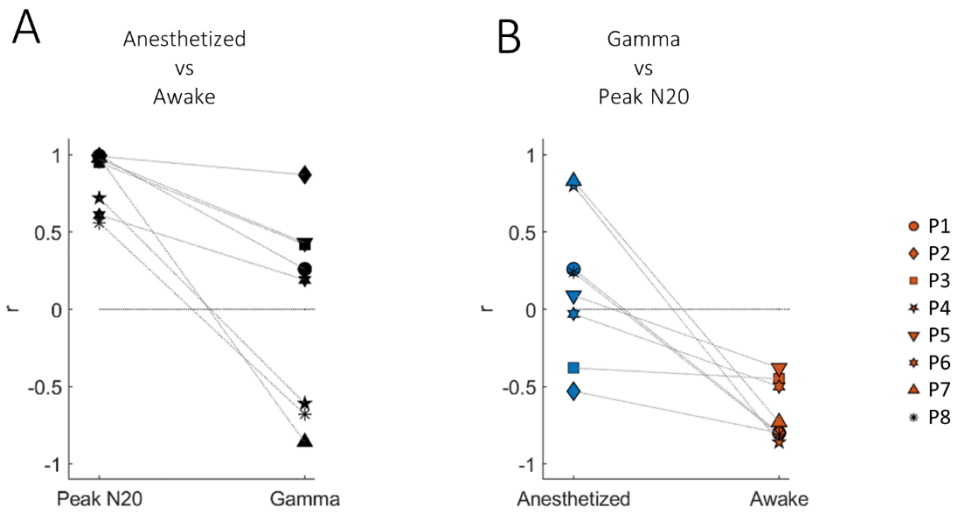
A
Anesthetized
vs
Awake
1
0.5
0
-0.5
-1
r
Peak N20
Gamma
B
Gamma
vs
Peak N20
1
0.5
0
-0.5
-1
r
Anesthetized
Awake
P1
P2
P3
P4
P5
P6
P7
P8

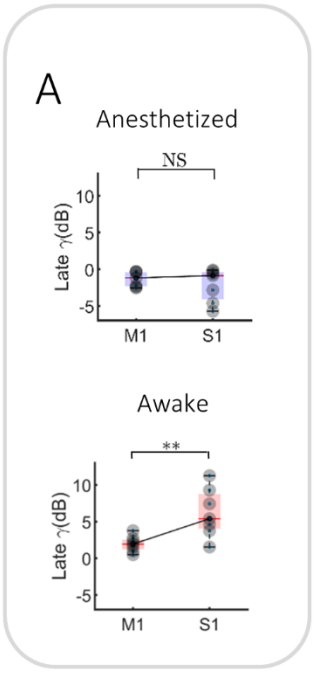
A
Anesthetized
NS
Late γ(dB)
10
5
0
-5
M1
S1
Awake
**
Late γ(dB)
10
5
0
-5
M1
S1

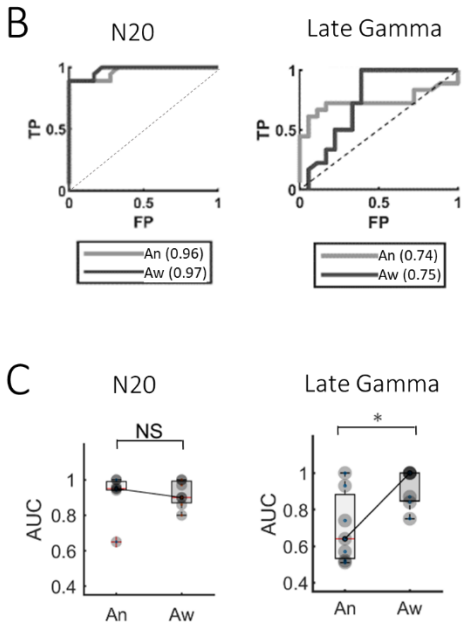
B
N20
Late Gamma
TP
FP
0
0.5
1
An (0.96)
Aw (0.97)
An (0.74)
Aw (0.75)
C
N20
Late Gamma
NS
*
AUC
0.4
0.6
0.8
1
An
Aw

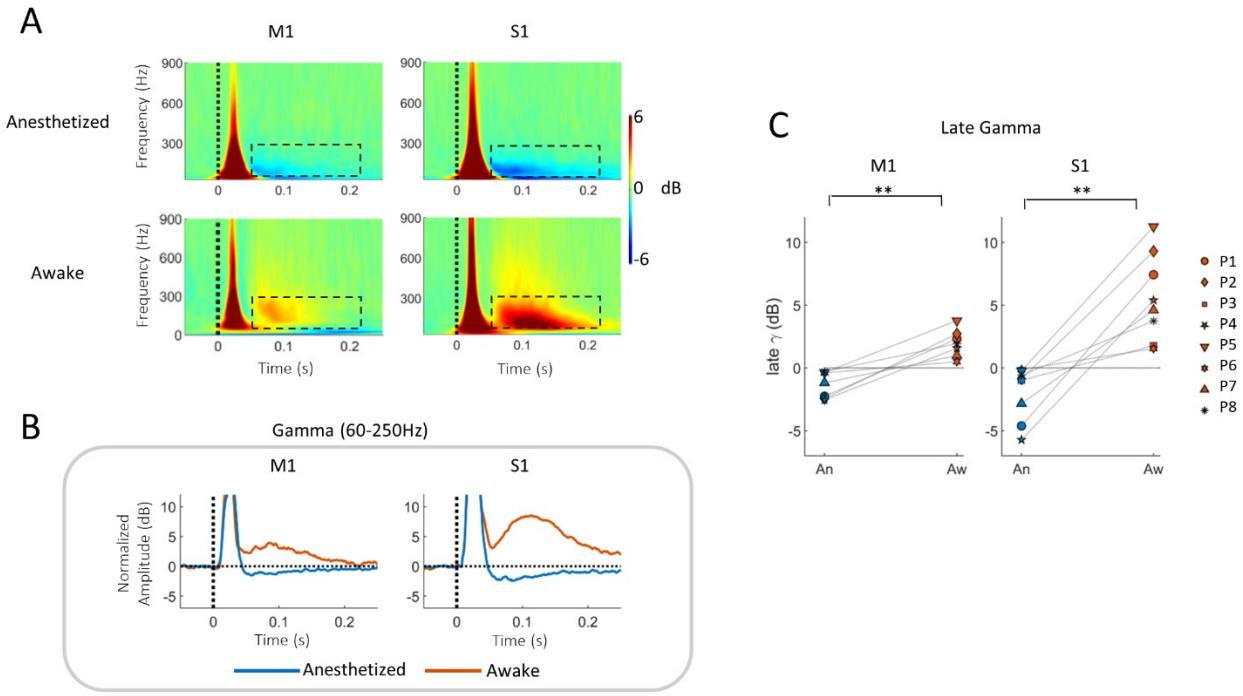
A
M1
S1
Anesthetized
Awake
Frequency (Hz)
900
600
300
0
0.1
0.2
Time (s)
6
0
-6
dB
B
Gamma (60-250Hz)
M1
S1
Normalized Amplitude (dB)
10
5
0
-5
Time (s)
Anesthetized
Awake
C
Late Gamma
M1
S1
**
late γ (dB)
An
Aw
P1
P2
P3
P4
P5
P6
P7
P8